ELSEVIER

Journal of Alloys and Compounds 434–435 (2007) 756–759

Journal of ALLOYS AND COMPOUNDS

www.elsevier.com/locate/jallcom

Effect of transition metal additions on the electrochemical properties of a MgNi-based alloy

S.F. Santos [a,*], J.F.R. de Castro [a], T.T. Ishikawa [b], E.A. Ticianelli [a]

[a] *Institute of Chemistry of São Carlos, University of São Paulo, Av. Trab. São-Carlense no. 400, CP 780, São Carlos, SP, CEP 13560-970, Brazil*
[b] *Department of Materials Engineering, Federal University of São Carlos, Rod. Washington Luís Km 235, São Carlos, SP, CEP 13565-905, Brazil*

Available online 29 September 2006

Abstract

Mg–Ni metastable alloys (amorphous and/or nanocrystalline) are promising candidate materials to be used as anode in Ni–MH batteries. In the present work, Mg–50 at.% Ni and Mg–45 at.% Ni–10 at.% TM alloys (where TM = Co, Zr, V, Cr, Ti and Nb transition metals) were processed for 72 h of mechanical alloying in a planetary ball mill. After milling, the alloys were characterized by X-ray diffraction and submitted to galvanostatic cycles of charge and discharge. All samples were nanostructured and presented the highest discharge capacity at the 1st cycle. The Zr, Cr and Nb alloying elements increased the maximum discharge capacity from 221 mA h/g (of the binary alloy) to 293, 246 and 276 mA h/g, respectively. Additions of Co and Ti decreased the maximum discharge capacity to 136 and 117 mA h/g, respectively. Concerning the cycle of life of the electrodes, the best results were obtained for the Mg–Ni–Cr and Mg–Ni–Co alloys.

Keywords: Nanostructured materials; Hydrogen absorbing materials; Mechanical alloying

1. Introduction

Since 1989, nickel-metal hydride rechargeable batteries have been commercially produced [1]. The demand for batteries with higher densities of energy has motivated the development of new hydrogen storage materials for electrochemical applications [2–4]. In this scenario, Mg–Ni metastable alloys (amorphous and/or nanocrystalline) are attractive candidates due to their large hydrogen storage capacities, light weight and low cost when compared to others hydrogen storage materials [4,5].

In the recent years, it was found that Mg–Ni based alloys processed by mechanical alloying (MA) have a large discharge capacity and surface activity during electrochemical tests [4–6]. Nevertheless, the poor cyclic performance, i.e. low cyclic life, of these alloys has hindered their utilization in commercial batteries. Further to MA, addition of alloying elements has been investigated as a useful way to obtain electrodes with improved performance [4–11].

In the present work, it was investigated the influence of the transition metal (TM) additions (10 at.% of TM) on the structure and electrode performance of Mg–Ni based alloys processed by mechanical alloying. The composition of these ternary alloys was established in view of maintain the 1:1 atomic ratio between Mg and Ni. The adoption of this alloy design criteria was motivated by some reports stating the large discharge capacity of the Mg–50 at.% Ni alloy [12,13].

2. Experimental procedure

The Mg–50% Ni and Mg–45% Ni–10% TM (TM = Co, Cr, Nb, Ti, V and Zr) alloys (in at.%) were processed by mechanical alloying with high purity starting materials. The processing of these alloys was carried out using a Fritsch P7 planetary ball mill. Stainless steel vials were specially designed to permit the air evacuation and argon introduction. The same processing conditions were used for all alloys, i.e.: Ball to powder weight ratio of 15:1, argon atmosphere and 72 h of milling. After milling, the samples were handled in a glove-box under Ar to minimize the oxidation of the powders.

The samples were structurally characterized by X-ray diffraction (XRD) with Cu Kα radiation using a Siemens D5005 diffratometer.

The electrodes were prepared by cold pressing a mixture of 0.1 g of the alloy powders with 0.1 g of a blend of carbon black (Vulkan XC-72R) with 33 wt.% of polytetrafluoroethylene (PTFE) binder in both sides of a Ni screen with an area of 2 cm^2. The electrochemical measurements were carried out in a three electrode cell, with a Pt counter electrode, an Hg/HgO reference electrode and a 6 mol L^{-1} KOH electrolyte. The density of charge of the electrodes was 50 mA/g of active material and the discharge density was 20 mA/g. The cut-off potential was −0.65 V (*versus* Hg/HgO, KOH-6 mol L^{-1}).

* Corresponding author: IRH – UQTR, 351 boul. des Forges, C.P.500, Trois-Rivières, QC, Canada, G9A5H7.
E-mail address: sfsantos91@yahoo.com.br (S.F. Santos).

0925-8388/$ – see front matter © 2006 Elsevier B.V. All rights reserved.
doi:10.1016/j.jallcom.2006.08.153

3. Results and discussion

Figs. 1 and 2 show the curves of discharge capacity (mA h g^{-1}) *versus* cycle number for the investigated alloys. All samples presented the maximum discharge capacity at the first cycle, indicating the activated state of the alloys. Further cycles of charge/discarge promoted decay in these curves. The maximum discharge capacity of the binary MgNi alloy was 221 mA h g^{-1}. The additions of Zr, Nb and Cr resulted in an increase of the maximum discharge capacity from 221 to 293, 276 and 246 mA h g^{-1}, respectively. In the case V, the maximum discharge capacity was practically the same of the binary alloy (i.e. 223 mA h g^{-1}) and a reduction of the maximum discharge capacity occurred when Ti and Co were added (117 and 136 mA h g^{-1}, respectively).

Table 1 shows the values of maximum discharge capacities and the parameters of cycle life for the studied alloys. The cycle life of the electrodes was evaluated by the attenuation coefficient (k_n) and average attenuation coefficient (k_{ave}) which are defined,

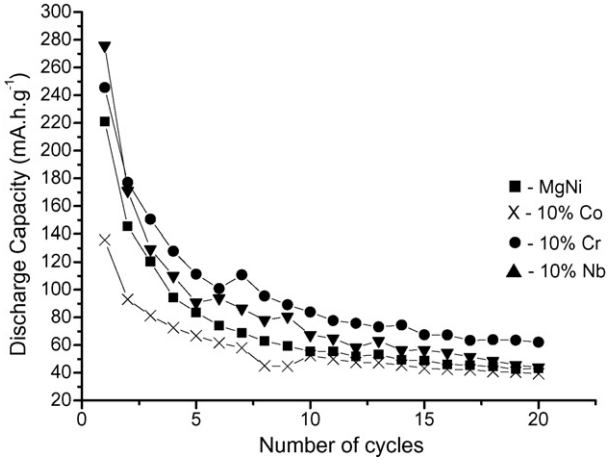

Fig. 1. Discharge capacity as a function of the number of cycles of the Mg–Ni, Mg–Ni–Co, Mg–Ni–Cr and Mg–Ni–Nb alloys.

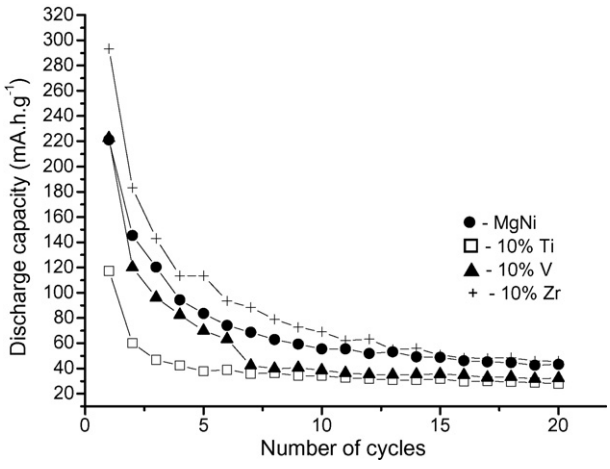

Fig. 2. Discharge capacity as a function of the number of cycles of the Mg–Ni, Mg–Ni–Ti, Mg–Ni–V and Mg–Ni–Zr alloys.

Table 1
Maximum discharge capacities and cycle life parameters of the alloy electrodes

Alloy	C_{max} (mA h/g)	k_5	k_{10}	k_{20}	k_{ave}
Mg–Ni	221	0.378	0.251	0.196	0.275
Mg–Ni–Co	136	0.453	0.342	0.252	0.349
Mg–Ni–Cr	246	0.491	0.385	0.289	0.388
Mg–Ni–Nb	276	0.329	0.244	0.159	0.244
Mg–Ni–Ti	117	0.306	0.293	0.239	0.279
Mg–Ni–V	223	0.314	0.173	0.145	0.210
Mg–Ni–Zr	293	0.387	0.235	0.156	0.259

in the present work, as

$$k_n = \frac{C_n}{C_{max}} \quad (1)$$

where C_n is the discharge capacity at the nth cycle of charge/discharge and C_{max} is the maximum discharge capacity of the electrode, and

$$k_{ave} = \frac{k_5 + k_{10} + k_{20}}{3} \quad (2)$$

Figs. 1 and 2 show the decay of the curves of discharge capacity as a function of the number of cycles. These data were also presented in a quantitatively form in Table 1. The additions of Co and Cr softened the decay of the discharge capacity *versus* number of cycles (k_{ave} increased from 0.275 to 0.349 and 0.388, respectively). The addition of Ti do not exerted an appreciable effect on the cycle life. In the case of Nb, Zr and V, a decrease of the cycle life was observed (k_{ave} decreased from 0.275 to 0.244, 0.259 and 0.210, respectively). The alloys which presented highest discharge capacities also had the poorest cyclic performances. This behavior had two exceptions which are Cr and V additions. The former presented improvement in both maximum discharge capacity and cyclic stability when compared to the binary alloy while V presents almost the same discharge capacity of the binary alloy and the poorest cyclic stability of all investigated alloys.

Figs. 3 and 4 show the X-ray diffraction patterns of the binary and ternary alloys. Notwithstanding the relative long milling time of mechanical alloying (72 h), the samples still presented diffraction peaks, which are broadened due to the decreased crystallite sizes and presence of residual stresses. The XRD patterns also exhibited a change of the base lines which matches well to amorphous bands. This behavior is more pronounced in the Mg–Ni and Mg–Ni–Nb diffraction patterns (Fig. 3). As expected, it was only detected diffraction peaks of the Mg_2Ni and $MgNi_2$ intermetallics for the binary alloy. For the Mg–Ni–Cr alloy, only the diffraction peaks of Mg_2Ni and $MgNi_2$ can be clearly observed. Nevertheless, the main diffraction peaks of Cr and $MgNi_2$ are close and can be overlapped due to the peaks broadening. In the case of Mg–Ni–Co and Mg–Ni–Nb, in addition to the diffraction peaks of Mg_2Ni and $MgNi_2$ phases, peaks of Co and Nb can also be detected, respectively (Fig. 3).

Fig. 4 shows the XRD patterns of the Mg–Ni, Mg–Ni–Ti, Mg–Ni–V and Mg–Ni–Zr alloys. In the same way of the previously discussed XRD patterns, in Fig. 3, these patterns also presented broadened diffraction peaks and the presence of an

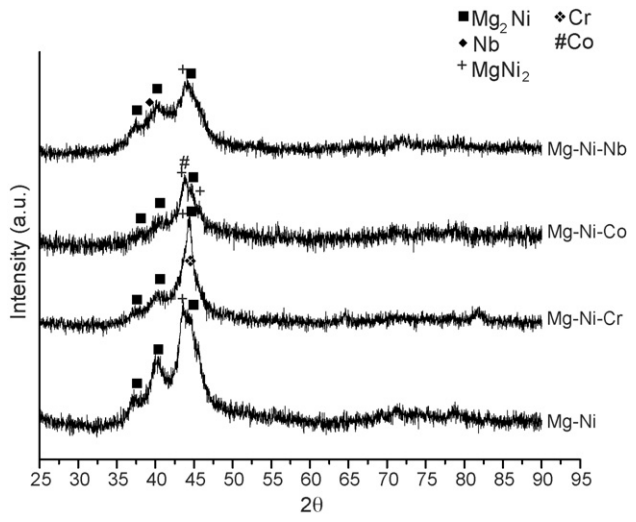

Fig. 3. XRD patterns of the Mg–Ni, Mg–Ni–Cr, Mg–Ni–Co and Mg–Ni–Nb alloys.

amount of amorphous phase cannot be disregarded. For the Mg–Ni–Ti alloy, the Mg_2Ni, $MgNi_2$ and Ni_3Ti intermetallic phases were detected. In the case of Mg–Ni–V, the detected phases were Mg_2Ni, $MgNi_2$, V and Ni_2V_3. Finally for the Mg–Ni–Zr alloy, the detected phases were Mg_2Ni, $MgNi_2$, Zr_2Ni_7 and Zr.

The complex nanostructure of these multi-phase alloys, here studied, makes difficult the correlation between electrochemical performance and structure. Nevertheless, it can be observed that the maximum discharge capacity seems to be related to the intensity of the Mg_2Ni diffraction peak of the alloys, i.e. the amount of this phase. Besides the quantitative errors involved with the correlation between the intensity of a diffraction peak and the amount of the corresponding phase without a more precise approach, in a qualitative point of view, the intensity of the main peak of the Mg_2Ni phase can reasonably explain the discharge capacity behavior of the investigated alloys. Taken Mg–Ni–Zr and Mg–Ni–Ti as examples, it can be observed that

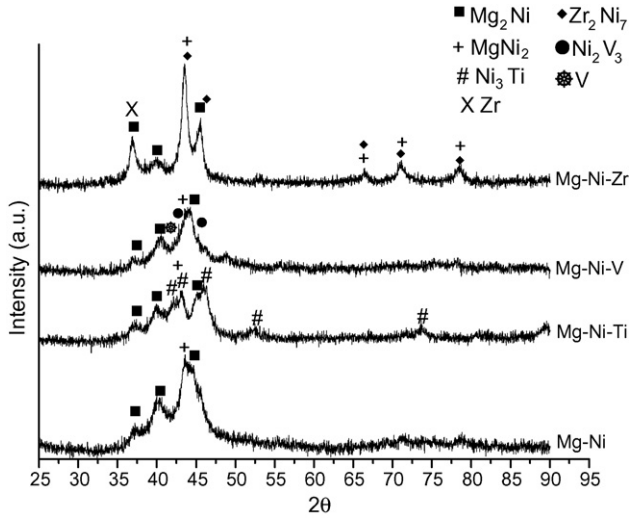

Fig. 4. XRD patters of the Mg–Ni, Mg–Ni–Ti, Mg–Ni–V and Mg–Ni–Zr alloys.

these alloys presented the largest and lowest intensities of the Mg_2Ni main diffraction peak and the largest and lowest maximum discharge capacities, respectively.

The values of the maximum discharge capacity of the investigated alloys are lower of some reported for Mg–Ni–TM ternary alloys [7,8]. The reason of this discrepancy is mainly related to the structure of the alloys. The best electrochemical properties reported for Mg–Ni–TM alloys were obtained for fully amorphous structures. In the case of Mg–Ni–Ti, which presented the lowest maximum discharge capacity in the present study, there is a large difference between the present electrochemical results and those previously reported (ranging from 150 to 580 mA h g^{-1}) [7]. This difference is related to the different chemical compositions and mainly to the different structures between the present studied alloys and those formerly reported [7]. In the present case, the Ni_3Ti intermetallic was formed during processing and it is probably related to the poor discharge capacity of this ternary alloy since this phase does not absorb hydrogen [14], and decreased the amount of Ni available for the formation of Mg_2Ni and amorphous Mg–Ni phases. In the case of this last phase, it is more easily formed when the amount of Ni is in the range of 50–70 at.% [15].

4. Conclusions

The addition of a transition metal third element caused strong modification of the electrochemical properties of the original Mg–50% Ni binary alloy. The additions of Zr, Nb and Cr improved the maximum discharge capacity of the electrodes from 221 to 293, 276 and 246 mA h g^{-1}, respectively, and the additions of Co and Ti decreased this property to 136 and 117, respectively. In the case of cycle life, the best results were obtained for Cr and Co additions which increased the k_{ave} parameter from 0.275 to 0.349 and 0.388, respectively. On the other hand, additions of Zr, Nb and V decreased the k_{ave} parameter to 0.259, 0.244 and 0.210, respectively.

The unique ternary alloy which improved both maximum discharge capacity and cycle life performance was the Mg–45% Ni–10% Cr and, due to this, can be considered the most successful ternary alloy here studied.

The electrochemical performance of the investigated ternary alloys is related to its complex multiphase nanostructures. These alloys presented poorest electrochemical performances when compared to some Mg–Ni–TM fully amorphous alloys reported on the literature.

Acknowledgements

The authors would like to acknowledge the Brazilian institutions FAPESP and CNPq for financial support.

References

[1] S.R. Ovshinsky, M.A. Fetcenko, App. Phys. A 72 (2001) 239.
[2] P.H.L. Notten, M. Ouwerkerk, H. van Hal, D. Beelen, W. Keurb, J. Zhou, H.J. Feil, J. Power Sources 129 (2004) 45.

[3] A. Taniguchi, N. Fujioka, M. Ikoma, A. Ohta, J. Power Sources 100 (2001) 117.
[4] J.J. Jiang, M. Gasik, J. Power Sources 89 (2000) 117.
[5] S.-C. Han, P.S. Lee, J.-Y. Lee, A. Zuttel, L. Schlapbach, J. Alloys Compd. 306 (2000) 219.
[6] H.Y. Lee, N.H. Goo, W.T. Jeong, K.S. Lee, J. Alloys Compd. 313 (2000) 258.
[7] S. Ruggeri, L. Roué, J. Huot, R. Schultz, L. Aymard, J.-M. Tarascon, J. Power Sources 112 (2002) 547.
[8] H. Ye, Y.Q. Lei, L.S. Chen, H. Zhang, J. Alloys Compd. 311 (2000) 194.
[9] W.-K. Choi, T. Tanaka, T. Morikawa, H. Inoue, C. Iwakura, J. Alloys Compd. 302 (2000) 82.
[10] H.-T. Yuan, L.-B. Wang, R. Cao, Y.-J. Wang, Y.-S. Zhang, D.-Y. Yan, W.-H. Zhang, W.-L. Gong, J Alloys Compd. 309 (2000) 208.
[11] A. Pasturel, J.L. Bobet, B. Chevalier, J. Alloys Compd. 356–357 (2003) 764.
[12] S.G. Zhang, Y. Hara, T. Morikawa, H. Inoue, C. Iwakura, J. Alloys Compd. 293–295 (1999) 552.
[13] T. Abe, S. Inoue, D. Mu, Y. Hatano, K. Watanabe, J. Alloys Compd. 349 (2003) 279.
[14] Y.-H. Xu, C.-P. Chen, Q.-D. Wang, Mater. Chem. Phys. 71 (2001) 190.
[15] S.J. Ji, J.C. Sun, Z.W. Yu, Z.K. Hei, L. Yan, Int. J. Hydrogen Energy 24 (1999) 59.